



Stromal Cells Promote Neovascular Invasion Across Tissue Interfaces

Hannah A. Strobel^{1†}, Steven A. LaBelle^{2,3†}, Laxminarayanan Krishnan⁴, Jacob Dale⁴, Adam Rauff^{2,3}, A. Marsh Poulson IV^{2,3}, Nathan Bader⁴, Jason E. Beare⁴, Klevis Aliaj^{2,3}, Jeffrey A. Weiss^{2,3*} and James B. Hoying^{1,4*}

¹ Advanced Solutions Life Sciences, Manchester, NH, United States, ² Department of Biomedical Engineering, University of Utah, Salt Lake City, UT, United States, ³ Scientific Computing and Imaging Institute, University of Utah, Salt Lake City, UT, United States, ⁴ Cardiovascular Innovation Institute, Department of Physiology, University of Louisville, Louisville, KY, United States

OPEN ACCESS

Edited by:

Tara Haas,
York University, Canada

Reviewed by:

Walter Lee Murfee,
University of Florida, United States
Andrew Benest,
University of Nottingham,
United Kingdom

*Correspondence:

Jeffrey A. Weiss
jeff.weiss@utah.edu
James B. Hoying
jhoying@advancedsolutions.com

[†] These authors have contributed
equally to this work

Specialty section:

This article was submitted to
Vascular Physiology,
a section of the journal
Frontiers in Physiology

Received: 17 June 2020

Accepted: 27 July 2020

Published: 14 August 2020

Citation:

Strobel HA, LaBelle SA, Krishnan L, Dale J, Rauff A, Poulson AM IV, Bader N, Beare JE, Aliaj K, Weiss JA and Hoying JB (2020) Stromal Cells Promote Neovascular Invasion Across Tissue Interfaces. *Front. Physiol.* 11:1026. doi: 10.3389/fphys.2020.01026

Vascular connectivity between adjacent vessel beds within and between tissue compartments is essential to any successful neovascularization process. To establish new connections, growing neovessels must locate other vascular elements during angiogenesis, often crossing matrix and other tissue-associated boundaries and interfaces. How growing neovessels traverse any tissue interface, whether part of the native tissue structure or secondary to a regenerative procedure (e.g., an implant), is not known. In this study, we developed an experimental model of angiogenesis wherein growing neovessels must interact with a 3D interstitial collagen matrix interface that separates two distinct tissue compartments. Using this model, we determined that matrix interfaces act as a barrier to neovessel growth, deflecting growing neovessels parallel to the interface. Computational modeling of the neovessel/matrix biomechanical interactions at the interface demonstrated that differences in collagen fibril density near and at the interface are the likely mechanism of deflection, while fibril alignment guides deflected neovessels along the interface. Interestingly, stromal cells facilitated neovessel interface crossing during angiogenesis via a vascular endothelial growth factor (VEGF)-A dependent process. However, ubiquitous addition of VEGF-A in the absence of stromal cells did not promote interface invasion. Therefore, our findings demonstrate that vascularization of a tissue via angiogenesis involves stromal cells providing positional cues to the growing neovasculature and provides insight into how a microvasculature is organized within a tissue.

Keywords: stromal cells, tissue interface, neovessel invasion, vascular biology, VEGF

INTRODUCTION

The process of angiogenesis is fundamental to the formation of new vasculatures during development (Breier, 2000; Nunes et al., 2013), tissue repair (Ravanti and Kahari, 2000), tumorigenesis (Folkman, 1995; Grant et al., 2002), and tissue engraftment (Laschke et al., 2006). One important, largely under-studied aspect of angiogenesis is the process by which growing

Abbreviations: ANOVA, Analysis of Variance; CIF, core-in-field; DMEM, Dulbecco's Modified Eagle Medium; GFP, green fluorescent protein; MV, microvessel; SD, Standard Deviation; SEM, scanning electron microscopy; SEM, standard error of the mean; SHG, second harmonic generation; SVF, stromal vascular fraction; VEGF, vascular endothelial growth factor.

neovessels navigate through complex tissue structures and stromal compartments in the adult. Here, a neovessel must cross a tissue interface comprised of structured matrix and cells to increase tissue vascularization or to engage with a perfused vascular unit. The latter role of the stroma as a potential barrier to neovessel growth and elongation is particularly relevant when new vascular connections are required to form between adjacent vascular beds, whether present in neighboring tissue compartments or between two distinct tissues. Effective neovascular invasion is perhaps most relevant to the vascularization of implanted tissues. Regardless of the type of implant, the microvasculatures of the implant and the surrounding host tissue must connect across the implantation interface to supply the implant or graft with blood. In the absence of this interface invasion, the implant/graft will become ischemic and fail.

It has been established that stromal matrix deformation, which arises from mechanical loading of a tissue and traction stresses generated by growing neovessels, has a strong influence over neovessel orientation and growth direction (Hoying et al., 2014). This reflects the ability of fibrils comprising the stromal matrix to deform, which is affected by fibril density (e.g., high density reduces compliance and thus deformation), cross-linking (reduces the ability of fibrils to translate and deform relative to each other), and fibril anisotropy (modifies proportion of fibrils engaged in tension). Dense, stiffer matrices promote longer, less branched, neovessels, and retard overall neovessel alignment with more global stromal deformation (Edgar et al., 2014a,b; Underwood et al., 2014). Matrix crosslinks enhance stiffness independent of density yet similarly improve vessel outgrowth and branching (Bordeleau et al., 2017). Fibril alignment similarly affects the microscale matrix stiffness and porosity (Taufalele et al., 2019). Thus, neovessel navigation through tissues likely involves the complex interplay of matrix architecture, mechanical environment, and the spatiotemporal distribution of angiogenic factors. The extent and nature of this interplay has yet to be defined in angiogenesis. Consequently, we explored neovessel guidance dynamics in a simplified model of tissue interfaces involving growing neovessels and a model collagen type I boundary.

To improve tissue vascularization and consequently the success of tissue implants, the mechanisms controlling neovessel invasion across tissue interfaces must be better understood. Toward this, we have created a novel *in vitro* model of a tissue interface, consisting of a high-density collagen layer, formed between two lower density collagen compartments. This system builds on our previous work utilizing intact microvessel (MV) fragments, isolated from adipose tissue, as an accurate *in vitro* angiogenesis model. These MVs, when embedded in collagen, will sprout from the parent fragments, grow, inosculate, and form a neovascular network (Hoying et al., 1996; Nunes et al., 2010). Here, we combined these MVs with our tissue interface system to create an *in vitro* model of neovascular interface invasion.

Surprisingly, growing neovessels do not spontaneously navigate across an interface between two matrix compartments. We determined the role of matrix fibril density and alignment to this neovessel deflection by combining experimental density

and alignment measurements at an interface with computational simulations of dynamic matrix:neovessel behavior. Furthermore, our experiments, which mimic the stromal cellular content *in vivo*, identified the importance of tissue stromal cells in enabling angiogenic neovessels to overcome the biophysical cues and invade across the interface. Interestingly, blocking vascular endothelial growth factor (VEGF) produced by the stromal cells abrogated neovessel invasion promoted by the cells. Yet, exogenous addition of VEGF, while stimulating angiogenesis, did not promote invasion in the absence of cells suggesting that spatiotemporal gradients of biochemical cues established by the cells is one means by which the cells promoted invasion. In addition to better understanding how neovasculatures are established in a tissue, these findings provide new insights into the dynamic role of tissue-resident stromal cells in tissue vascularization. These insights may have strong implications in regenerative medicine and angiogenesis-related pathologies.

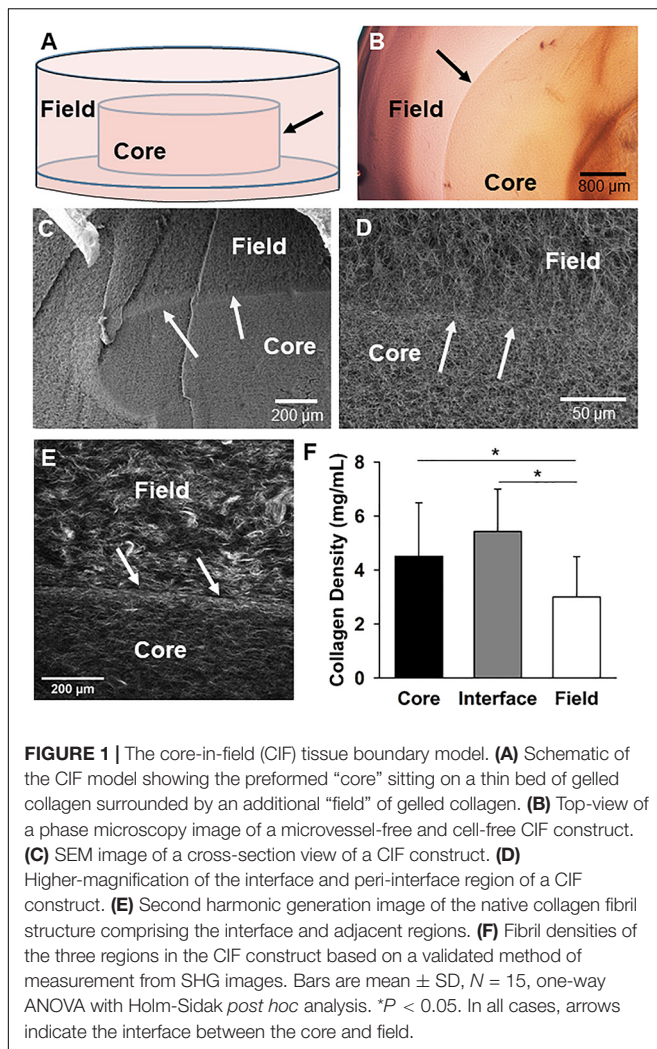
MATERIALS AND METHODS

Core-in-Field Model of Tissue Interfaces

An *in vitro* analog of tissue-tissue or tissue-implant boundaries was created using a “core-in-field” (CIF) model to examine the extent of vascular sprout outgrowth from the inner vascularized core region to the outer cell free region (**Figure 1**). Microvessel fragments were isolated from adult Sprague-Dawley rats by limited collagenase digestion and sequential filtration to remove single cells and retain only MVs (Chang et al., 2012). All tissue harvesting was approved by the Institutional Animal Care and Use Committee, and performed following euthanasia. The isolated MVs were suspended in 3 mg/mL collagen solution at a density of 60,000 MVs/mL of collagen solution. This vascularized collagen solution was first pipetted into wells (90 μ L/well) of a 96 well plate and gelled to create vascularized cores. The gelled, vascularized collagen cores were then transferred to wells of 48 well plates using a sterile transfer pipet, overlaid with another cell-free collagen solution (250 μ L/well), and gelled to envelop the vascularized core completely in cell-free collagen forming a “field” around the vascularized “core.” Dulbecco’s Modified Eagle Medium (DMEM) with 20% fetal bovine serum, 1% penicillin-streptomycin, 1% amphotericin-B was added to each construct once all was gelled (30 min at 37°C). Constructs were evaluated after 9–11 days.

Preparation and Use of Cells

Rat stromal vascular fraction (SVF) cells were harvested from epididymal fat pads of retired breeder Sprague-Dawley rats, or transgenic Sprague-Dawley rats in which all cells express GFP (SD-Tg(UBC-EGFP)1BaIRrrrc; RRRC, Missouri), as previously described (Nunes et al., 2013). Cells were used at 1×10^5 cells/mL collagen unless otherwise stated, which was previously determined as the maximum concentration of cells that did not promote rapid construct contraction (data not shown). Cells were either added with MVs to the construct cores only, or added instead to the field region only of the CIF construct (while MVs remained in the cores).



Soluble Factors

To test the effect of soluble VEGF on neovessel invasion, a recombinant VEGF-A₁₆₅ (Peprotech) was used at 10 ng/mL final concentration in the media. To trap VEGF in a separate experiment, a combination of recombinant human VEGF R1/Flt-1 Fc Chimera (321-FL/CF, R&D Systems) and recombinant human VEGF R2/KDRFlk-1 Fc Chimera (357-KD/CF, R&D Systems) was used at a final concentration in the media of 1 and 1.5 μ g/mL, respectively. The Fc chain of recombinant human IgG1 (110-HG, R&D Systems; 1.5 μ g/mL) was used as a control.

Assessment of Neovessel and Cellular Invasion

Following 9–11 days of culture, the number of neovessels that crossed the interface was counted for each sample. Images of the core were then taken and used to quantify total interface length using ImageJ¹. Locations where the interface was torn or

damaged were excluded from analysis. The number of crossing events for each sample is normalized both to interface length and vessel density. To calculate vessel density, constructs are first stained with Rhodamine labeled Lectin [Griffonia (Bandeiraea) Simplicifolia Lectin I (GSL I, BSL I), Vector Laboratories]. The entire core region was then imaged using confocal microscopy (Olympus FV3000 or Nikon A1R HD), and ImageJ was used to calculate vessel density of the outer region of the core, near the interface. Images were processed to improve contrast, thresholded to identify neovessels, filtered to remove single cells and debris from the foregrounds, and skeletonized. The average neovessel length density (total length of neovessels per area) was then measured using ImageJ. Data are reported for each group as

$$\frac{\# \text{crossing events} \div \text{interface circumference}}{\text{neovessel length density in the core}}$$

Cellular crossings were calculated by staining constructs with Hoechst dye, and imaging with a confocal microscope. Four images were taken from each sample, one at the top, bottom, left, and right of each sample. The number of nuclei in the field were counted using the cell counter in ImageJ, and this number was normalized to the area of the field region in the image.

All neovessel crossing experiments were repeated 3–5 times, by 2–3 separate investigators, with 3–5 samples per group. Bar graphs are represented as an average of the multiple experiments. A correction factor was employed to account for variation in vessel density between experiments. The corrected vessel density was used to normalize values for crossing events/interface length. In some cases, each experiment was plotted separately on the same graph in addition to overall means.

Image Acquisition and Collagen Characterization

Second harmonic generation (SHG) imaging was used to quantify collagen fibril density. Second harmonic generation images were acquired using a custom Prairie View Ultima multiphoton microscope (Bruker Corp). Images were acquired with 855 nm excitation and 435–485 nm detection using a high numerical aperture water immersion objective (APO-MP, 25X/1.1W, Nikon). Methods to determine the relationship between SHG signal intensity and collagen density are outlined in **Supplementary Figures S1–S3** and **Supplementary Data S1**.

Scanning electron microscopy (SEM) imaging was performed with FE-SEM/FIB field emission microscope (Tescan Lyra 3 GMU). Samples were cut in half and fixed overnight in 2.5% glutaraldehyde. They were then dehydrated with a graded series of ethanol, then critical point dried and sputter coated with 20–30 nm of gold/palladium prior to imaging.

Computational Modeling

Microvascular growth and neovessel guidance were simulated to determine the relative contributions of matrix density and fibril alignment to deflection at the interface. Matrix mechanics and the geometry of our experimental setup – two matrix compartments

¹<https://imagej.nih.gov/ij/>

partitioned by an interface – were represented in FEBio, an open-source finite element software² (Maas et al., 2012). FEBio solves for neovessel-induced matrix deformation, which determines local fibril alignment, and stress in the matrix. AngioFE, a plugin that couples neovascular growth and matrix mechanics (Edgar et al., 2012, 2014a,b, 2015a,b), was used in coordination with FEBio to simulate neovessel behavior and crossing at the interface in response to different matrix fibril densities and/or orientations. A detailed description of the modeling approach and parametric simulations can be found in **Supplementary data S2–S5** and **Supplementary Figures S4–S6**.

Statistical Analyses

Statistics were performed using SigmaPlot 11.0 (Systat). One-way ANOVA tests were used on pairwise multiple group comparisons of normal data, with a Tukey or Holm Sidak *post hoc* analysis where appropriate. On data that failed a Shapiro-Wilk normality test, a one-way ANOVA on Ranks with Newman-Keuls or Dunn's *post hoc* analysis was used. All other pairwise comparisons were analyzed by Student's *t*-tests. For all statistical comparisons, significance level $\alpha = 0.05$.

RESULTS

The “Core in Field” Model Contains a High-Density Collagen Interface

To investigate the mechanisms of neovessel invasion, we modified our proven isolated-MV angiogenesis model (Hoying et al., 1996; Nunes et al., 2010). In this model, intact MV fragments are embedded within a 3D collagen type I gel. When cultured, neovessels sprout and grow from the individual isolated parent MVs in a way that accurately recapitulates native angiogenesis (Hoying et al., 1996; Nunes et al., 2010; Utzinger et al., 2015). For these studies, we modified this model by establishing a “core” of collagen encased in a surrounding “field” of collagen with either compartment being free of or containing MVs and/or cells. A thin layer of condensed collagen forms as a visible interface between the core and field across which we can assess neovessel crossing/invasion. Construct biophysical features were characterized first without the addition of MVs to the core (**Figures 1A,B**), by imaging the collagen fibril structure at and adjacent to the interface. Scanning electron microscopy of the collagen structure indicated that the fibril structure from the core, across the interface, and into the field is heterogeneous with differences in both fibril structure and density (**Figures 1C,D**). Second harmonic generation imaging revealed the interface is comprised of a dense band of collagen relative to the less dense core and field regions, and circumferential fibril alignment at the interface was occasionally observed (**Figures 1D–F** and **Supplementary Figure S7**). These differences arose even though the starting collagen concentration used to make both the core and the field was 3 mg/mL.

Collagen Interfaces Deflect Angiogenic Neovessels, Blocking Interface Invasion

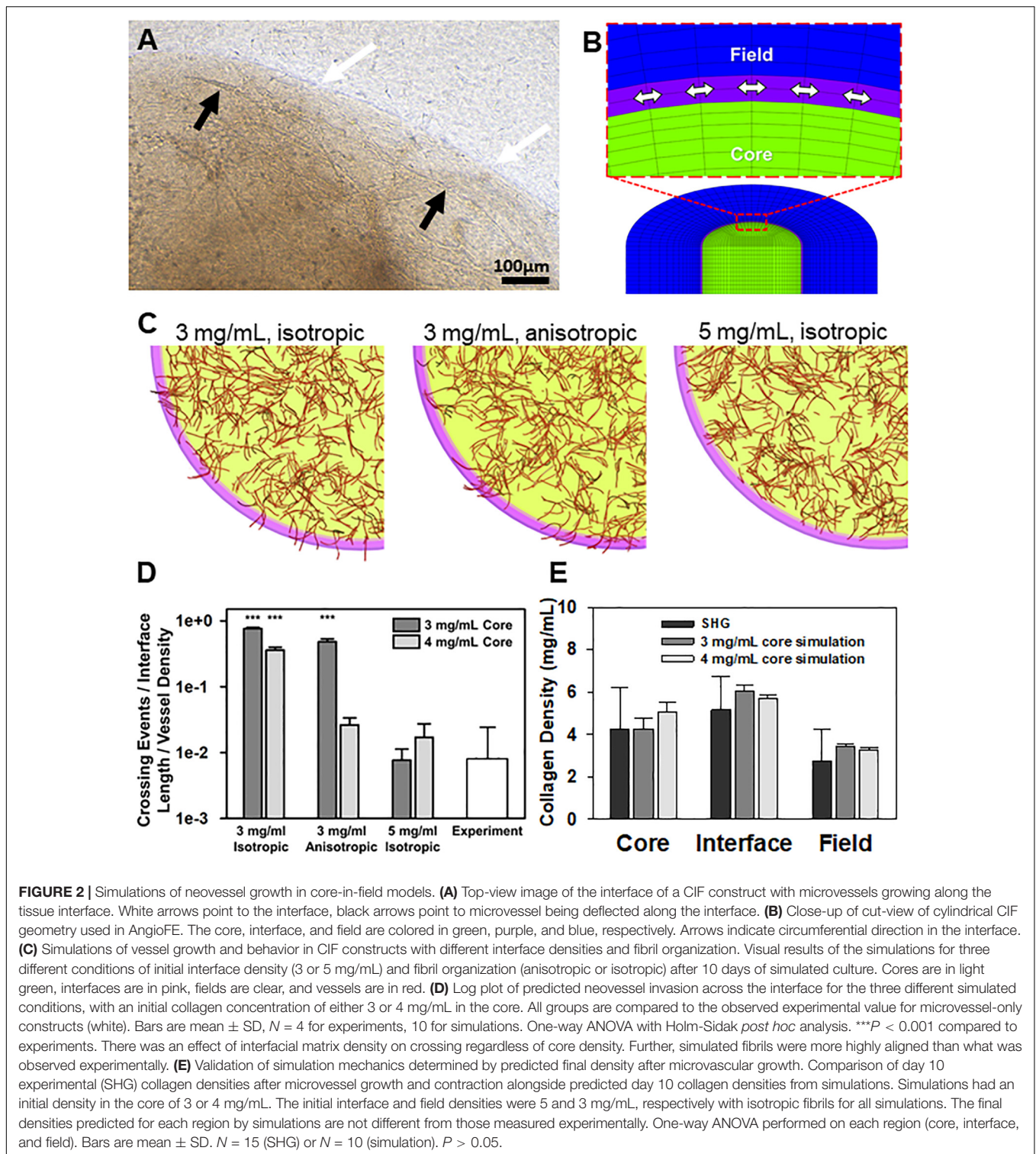
Surprisingly, when isolated MVs were included in the core at the time of casting and cultured for 7–10 days, growing neovessels were generally unable to spontaneously cross the collagen interface (**Figure 2A**). As neovessels approached the boundary, they were deflected laterally and continued to grow along the interface, but rarely across it. We have previously shown that growing neovessels are significantly influenced by the mechanics of the stromal environment in a dynamic, reciprocal fashion (Underwood et al., 2014; Utzinger et al., 2015). Specifically, the orientation of collagen fibrils realigns parallel to growing neovessels, the extent of which is affected by fibril density (Krishnan et al., 2008; Underwood et al., 2014). Based on these studies, we next used computational modeling to investigate if the deflection of growing neovessels was due to differences in fibril density and/or fibril alignment at the interface. Fibril alignment was assumed either isotropic or circumferentially aligned along the interface. Matrix density inputs in our models were determined from a multiple linear regression of SHG image intensity and acquisition parameters (**Supplementary Figures S1–S3** and **Supplementary Data S1**). Simulation setup is described in **Supplementary Data S2**.

In the simulations, neovessels robustly crossed in the absence of a high-density interface regardless of fibril orientation at the interface (**Figures 2B–D**). In contrast, increasing the interface density to 5 mg/mL reduced crossing to similar levels seen experimentally and, in some cases, prevented all neovessels from crossing the interface. Increasing the initial concentration of collagen in the core from 3 to 4 mg/mL reduced the extent of neovessel crossing (**Figure 2D**), partially reflecting the effect of higher collagen densities on neovessel growth in the core as well as the increase in collagen density at the interface due to contraction of the matrix by MVs (Edgar et al., 2014b). In all cases, high initial core matrix density or a high-density interface (due to polymerization or MV contraction) was required to prevent crossing. Neovessel mechanics were validated by comparing densities after 10 days of simulation with the experimental densities calculated from SHG image data after 10 days growth *in vitro* (**Figure 2E**, **Supplementary Figure S8**, and **Supplementary Data S1**). The simulations suggest that the condensed nature of the fibril network comprising the interface alone is sufficient to impede and deflect neovessel growth across the interface. Fibril anisotropy may contribute to the reduction in the frequency of crossing but is less potent in preventing invasion than matrix density. Fibril anisotropy does, however, encourage circumferential growth along the interface, a behavior observed experimentally after initial neovessel deflection (**Figure 2C** center).

Angiogenic Neovessel Interface Invasion Is Promoted by Stromal Cells

We have previously shown that implantation of MVs embedded in collagen results in rapid inosculation with the surrounding host circulation, progressing to form a new, perfused hierarchical microcirculation (Shepherd et al., 2004, 2007;

²www.febio.org



Gruionu et al., 2010; Nunes et al., 2010). In this situation, the vascular connections with the host circulation have been formed by neovessels that crossed the implant:host tissue boundary. To explain the contradictory lack of neovessel crossing in our *in vitro* system, we considered the possibility that host tissue resident

stromal cells at the implant site, which are absent in the *in vitro* CIF interface model, may be critical for mediating neovascular interface invasion in the implants. To test this possibility, we included SVF cells isolated from adipose in our *in vitro* invasion model. We chose adipose because it is a ready source of SVF

cells (Williams, 1995; Fraser et al., 2006; Zimmerlin et al., 2010) and SVF can improve lipoaspirate-grafting (Yoshimura et al., 2008), which we reasoned reflects an accelerated integration of graft vessels with the host circulation. Stromal vascular fraction contains the full spectrum of adipose stromal and vascular cells found in adipose tissue.

We tested two scenarios, one where SVF cells were mixed in the core region with the MVs, and one where SVF cells were located only in the field region adjacent to the MV-containing core. The inclusion of freshly isolated SVF cells in either the core or the field region promoted neovessel interface crossing (Figures 3A–C), although the effect was significantly higher when cells were located in the field region than the core (Figure 3C). As a follow up study, we tested the effect of cell number (Figure 3D). Initially, SVF cells were incorporated at a concentration of 10^5 cells/mL. However, because the field contains a greater volume than the core, there was a higher total number of cells present when SVF cells were incorporated into the field. To explore the possible effect of cell number, we tested starting SVF cell numbers in the core at both 100k and 250k cells per mL (corresponding to a total cell number of 10k and 25k cells per compartment) and compared that to SVF cells in the field at 40k or 100k per mL (corresponding to 10k or 25k cells per compartment). While increasing the total cell number in the core did increase crossing events, the effect was not as large as having SVF cells in the field. Having 25k total cells in the core was comparable to having 10k total cells in the field (Figure 3D). This suggests that both cell number and cellular spatial positioning have a role in neovessel invasion and guidance during angiogenesis.

Neovessels and Stromal Cells Do Not Grossly Alter Interface Structure

After observing that neovessel crossing is promoted by SVF cells, we began to evaluate possible mechanisms for this effect. We first considered the possibility that the cells remodeled or altered the collagen fibril interface to permit neovessel crossing. However, examination of the interface by SHG microscopy indicated no significant change in gross fibril density due to the presence of growing neovessels and/or SVF cells (Figure 4A and Supplementary Data S1). Nor were there any gross alterations to the interface such as gaps or fragmentation when imaged by SEM, although small holes were visible where cells and/or MVs crossed the interface (Figures 4B–D). Fibril anisotropy for each region (core, interface, and field) did not change with the inclusion of MVs or SVF cells (Supplementart Data S6 and Supplementary Figure S9). All of this suggests that the neovessels and SVF are not profoundly altering interface structure. However, subtle changes to the interface such as clipped cross-links between fibrils or micro-scale gaps between fibril bundles that might promote neovessel crossing cannot be ruled out as these may not be detected by either SHG or SEM imaging.

SVF Cells Migrate Across the Interface

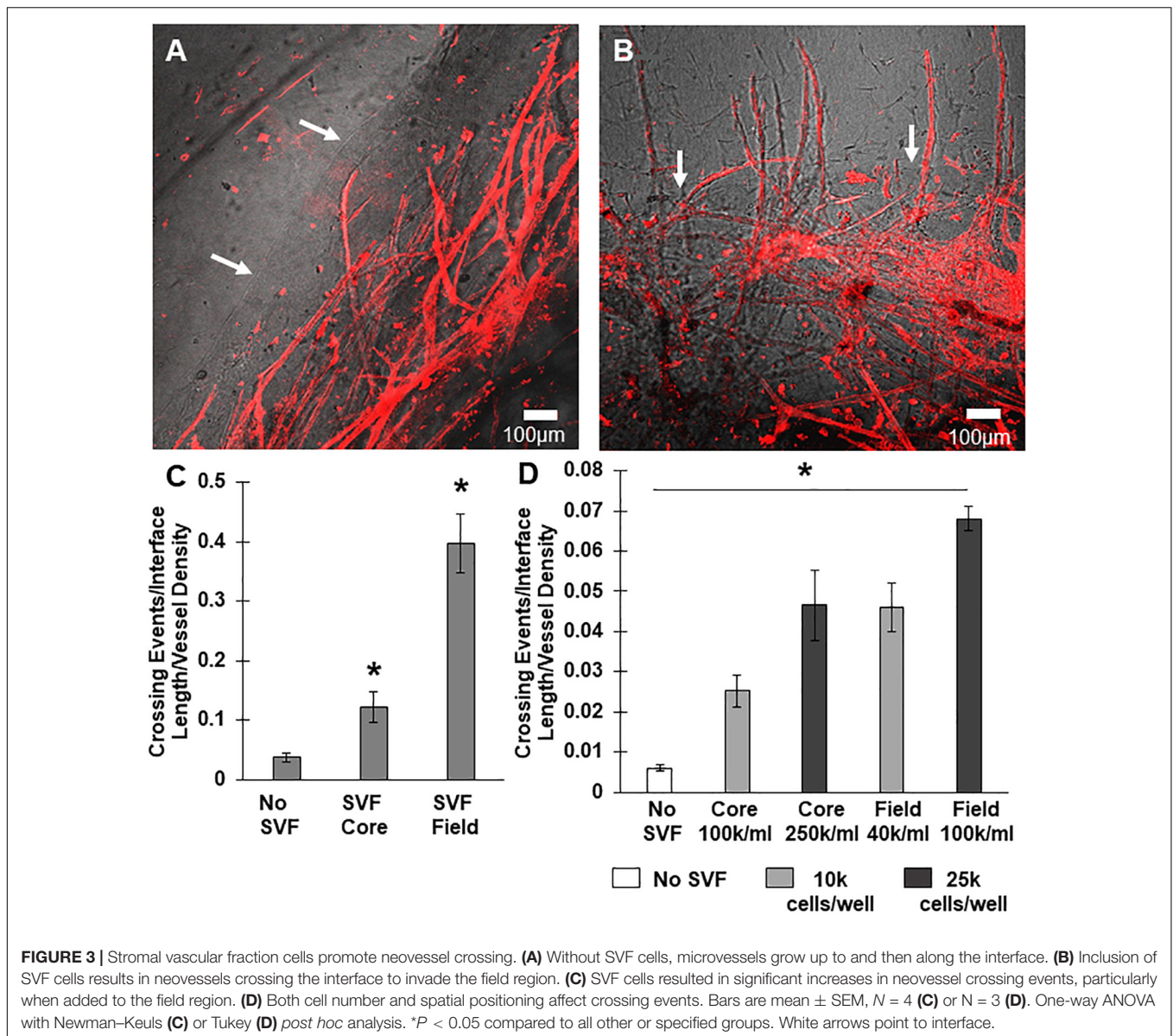
We also considered the possibility that the SVF cells could promote neovessel invasion by forming new vessel elements

across the interface *de novo*, via a vasculogenic-like process. Similar cell preparations can assemble into vessel-like elements when implanted (Koh et al., 2011; Maijub et al., 2014; Ramakrishnan et al., 2016). To test this hypothesis, we incorporated green fluorescent protein (GFP) positive SVF cells into cores with MVs that were not GFP+. Indeed, SVF cells incorporated into growing neovessels, including assembling onto the tip of a growing neovessel (Figures 5A,B). Additionally, there were not neovessels comprised entirely of SVF cells. Importantly, some neovessels that crossed the interface did not have any SVF cells incorporated into their structure. Therefore, while SVF cells do incorporate into growing neovessels, this incorporation does not appear necessary for the pro-invasive neovessel behavior. Interestingly, the findings suggest that in the presence of angiogenic vessels, SVF cells may preferentially add to the growing neovessel instead of *de novo* assembly of neovessels (crossing an interface or otherwise).

To confirm that SVF seeded in the core migrates from the core to the field, we stained constructs with nuclear Hoechst dye and counted cells that had crossed the interface. We previously observed that cells migrate across the interface regardless of presence of SVF, as some single cells remain in the MV isolation, and some leave the MVs after seeding. The number of cells that crossed the interface was much higher when SVF is incorporated within the core than with no SVF (Figures 5C–E). This indicates that the SVF is migrating across the interface, which may be a mechanism for MV crossing events. The cellular composition of SVF is likely different from those single cells migrating off of the individual MVs, which may explain why isolated cells alone do not have this effect while added SVF cells do.

VEGF-A Mediates Stromal Cell-Promoted Neovessel Invasion

Unlike the neovessels, we observed that SVF cells were not impeded by the interface as they readily migrated out of the core into the field. The absence of noticeable interface remodeling by the SVF cells and the irrelevance of cell attachment to the neovessel on pro-invasive activity suggests that the SVF cells provided a guidance cue, enabling the neovessels to overcome the deflective influence of the interface biophysical features. With this in mind, we tested the effect of soluble Flt/Flk receptor chimeras, to sequester VEGF-A, a potent vascular guidance cue (Gerhardt and Betsholtz, 2005). VEGF-A is highly expressed in SVF cells cultured in collagen gels (Supplementary Figure S10). In the presence of the VEGF-A trap, neovessel invasion stimulated by SVF cells was attenuated (Figure 6A), suggesting that SVF mediates neovessel invasion via VEGF-A signaling. While this result was not significant, the VEGF trap brought crossing events close to zero consistently across multiple experiments. The VEGF trap did not have a significant effect on overall vessel growth (Figure 6B). An IgG chimera control for the VEGF trap did show some inhibitory effect on crossing events, but this effect was not nearly as large as the VEGF trap itself. Unexpectedly, when VEGF-A alone (without SVF cells) was added exogenously to MV interface cultures, we did not observe a significant increase in interface crossing, despite the stimulation of higher

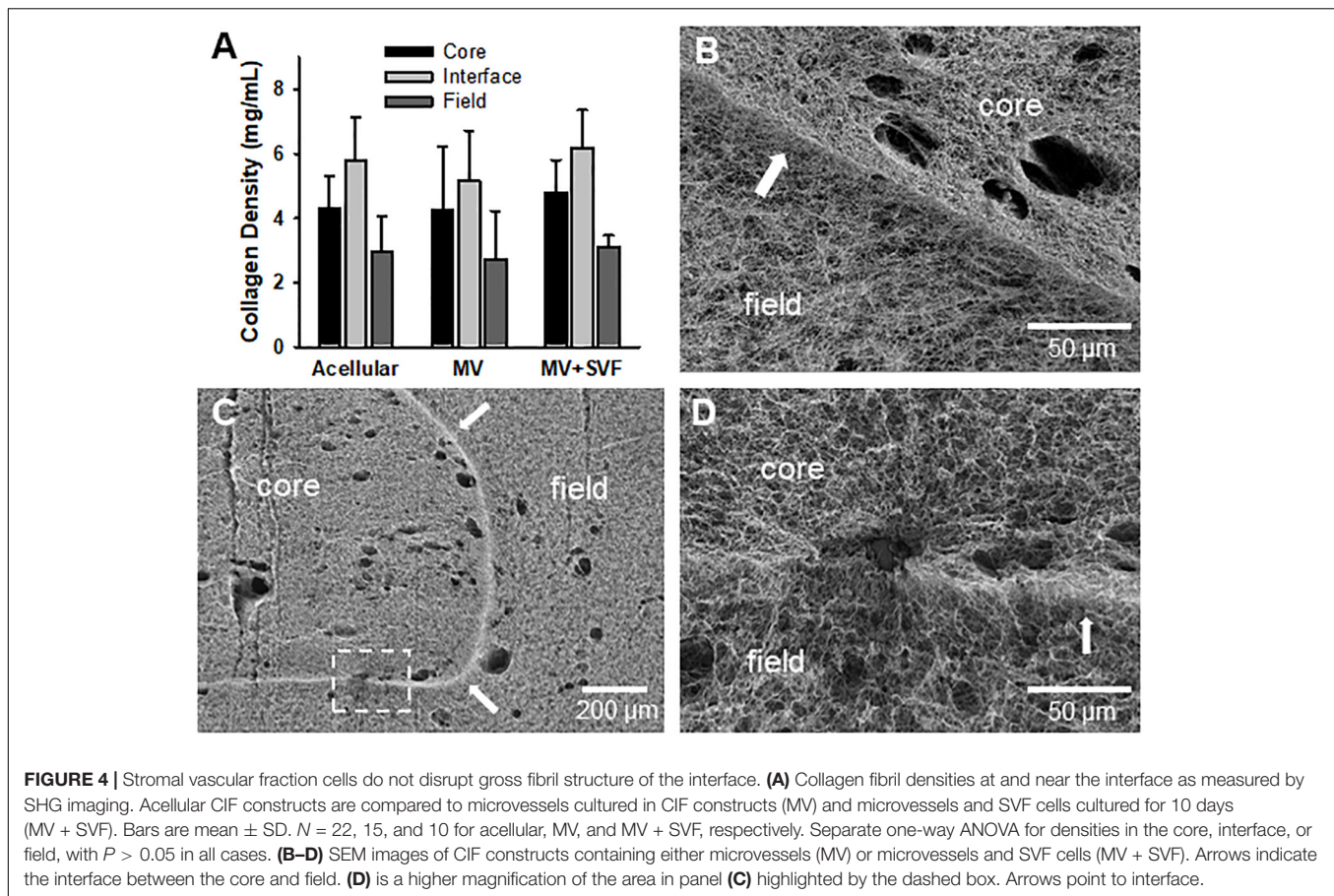


vessel densities (**Figures 6C,D**). Thus, despite exogenous VEGF-A promoting angiogenesis in the model, it did not promote more crossing events. These results suggest that it may be a gradient of VEGF-A, rather than its ubiquitous presence, that promotes neovessel interface crossings. To further test this, we compared the presence of SVF in the core or field to SVF in both the core and field. We hypothesized that this would eliminate any gradient of secreted/deposited VEGF between the core and the field, and consequently result in fewer neovessel crossings. We observed that crossings were comparable to the group with SVF in the core only. Having SVF in the field only still had the greatest effect (**Figure 7**). While sequestration of VEGF influenced SVF cell-mediated neovessel invasion, it is unlikely that VEGF is the sole factor governing angiogenesis in our model as other angiogenic and guidance factors are produced by the MV isolate and SVF cells (Rehman et al., 2004; Altalhi

et al., 2017). Furthermore, the VEGF trap employed, which utilizes VEGF-R1 and -R2 ligand binding domains, can also sequester the potent angiogenic placental growth factor (PLGF) (Luttun et al., 2003).

DISCUSSION

Here, we developed a novel *in vitro* model system for studying neovessel invasion across tissue interfaces. This system utilizes isolated MV fragments, which we have demonstrated can accurately recapitulate native angiogenesis. The model contains two collagen compartments, a “core” and a “field,” with a high collagen density interface layer between them. With this model, we initially observed that angiogenic neovessels are unable to cross the dense collagen interface. This was surprising,



given our previous observations that neovessels readily cross such interfaces *in vivo* (Shepherd et al., 2004, 2007; Gruionu et al., 2010; Nunes et al., 2010). Regardless, the finding that neovessels alone do not cross an interface prompted us to explore further the mechanisms that lead to neovessel invasion across tissue interfaces.

We explored the possibility that interface fibril density and orientation influence neovessel crossing behavior similar to that observed with tumor cells invading into matrix compartments (Han et al., 2016). Using SHG imaging, we determined that interface fibrils were compacted relative to those in the core and field. It was not clear, though, if the fibrils were also aligned in any orientation. To separate the potential influence of fibril density from alignment at the interface, we performed computational simulations that model the mechanical interactions between growing neovessels and the deformation of the matrix (AngioFE). When the simulated density (mimicking compaction) of the interface layer between the two compartments was high relative to the bulk core and field compartments, neovessel crossing events were infrequent, matching those observed experimentally. Unlike in the experiments, though, the neovessels did not grow along the interface in this simulation. In contrast, neovessel crossing events in the simulations were more frequent when fibrils at the interface were circumferentially aligned and not compacted. Interestingly, simulated neovessels grew along this

aligned interface. It's important to note that the simulated fibrils were idealized as being entirely aligned at the interface (a likely more extreme case than in the experiments). Overall, our simulations demonstrated that the condensed nature of the fibril network comprising the collagen:collagen interface is sufficient to impede neovessel growth across the interface. Circumferential fibril anisotropy does not appear to be primarily responsible for deflection at the interface but could be involved in directing neovessel growth along the interface. In bulk phase, collagen density and fibril alignment provide contact guidance cues for growing neovessels resulting in differences in neovessel growth rates, branching, and growth direction (Kirkpatrick et al., 2007; Edgar et al., 2014a; Underwood et al., 2014; Utzinger et al., 2015). Our findings highlight different possible roles of fibril alignment during invasion, as well, which may depend on the relative orientation of fibrils at the tissue boundary, cell type, and differences in matrix composition and density on each side of the interface.

Interestingly, the presence of tissue stromal cells (isolated from adipose) promoted neovessel invasion through the interface into the neighboring collagen compartment. This raised the possibility that stromal cells were remodeling the collagen interface such that it no longer served as a deflective barrier to the neovessels. As the density of collagen fibrils is critical in neovessel guidance (Underwood et al., 2014), degradation may facilitate neovessel

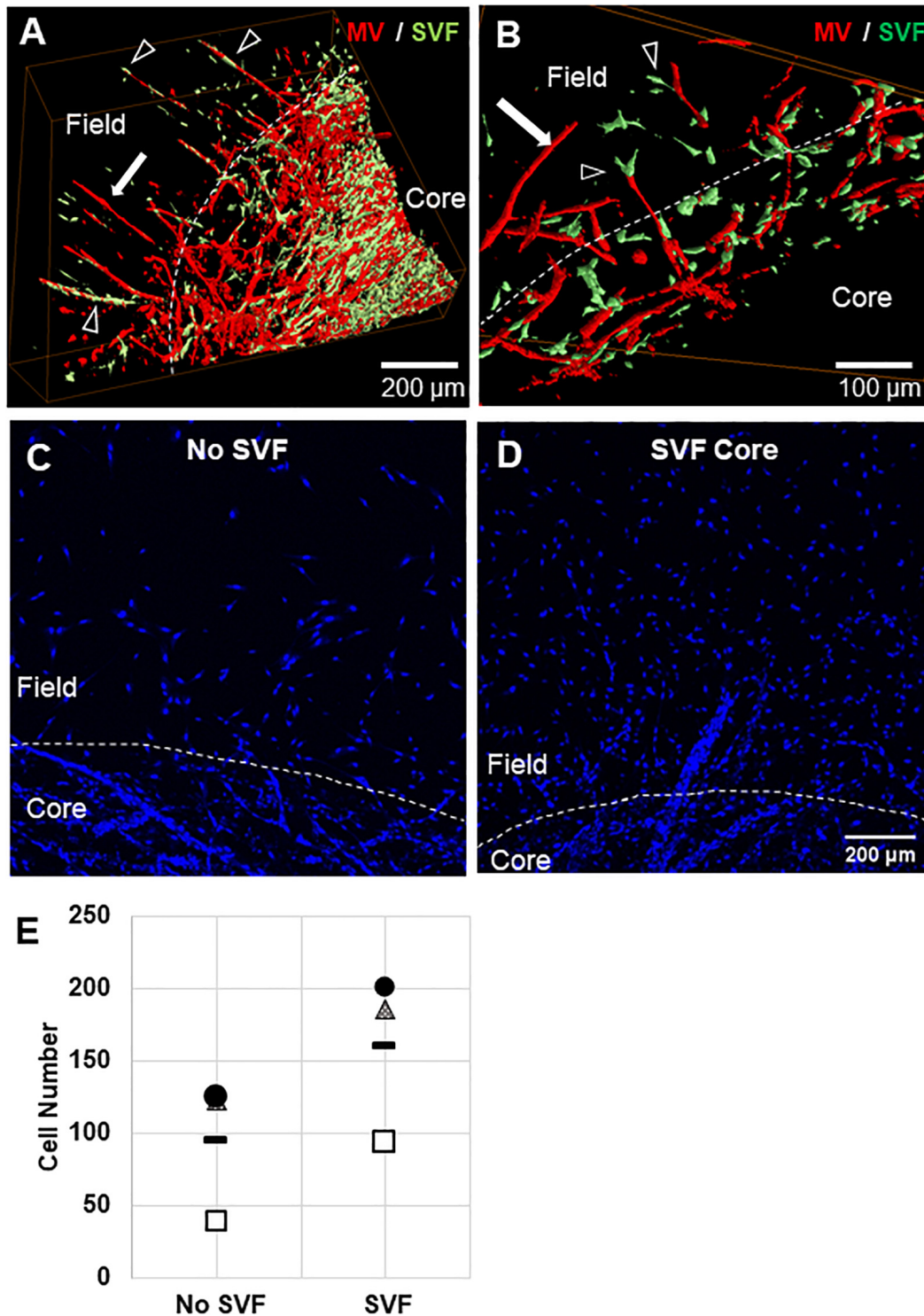


FIGURE 5 | Stromal cell migration from the core to the field. **(A,B)** Confocal image stacks of CIF constructs formed with microvessels (red, rhodamine labeled Lectin stain) and SVF cells (green, GFP+) in the core after 10 days of culture. **(C,D)** Images of Hoechst stained samples without **(C)** or with **(D)** SVF incorporated into the core region. **(E)** Graph of Hoechst stained cells counted in the field region after 10 days of culture, with or without initial SVF incorporation in the core region. The circle, triangle, and box each represent a different experiment, with the line representing the mean of the experiments. Each experiment was statistically evaluated individually using a student's *t*-test. $P < 0.05$ within the circle experiment and square experiment, but not the triangle experiment. In **(A–D)**, white arrows point to microvessels, black arrows point to SVF. White dashed line indicates the interface.

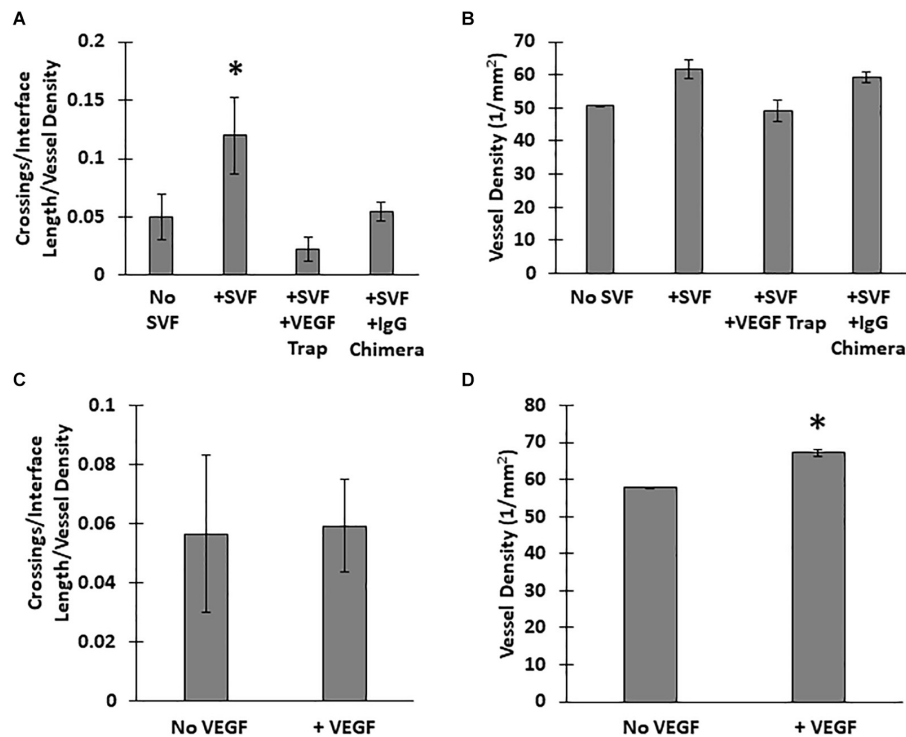
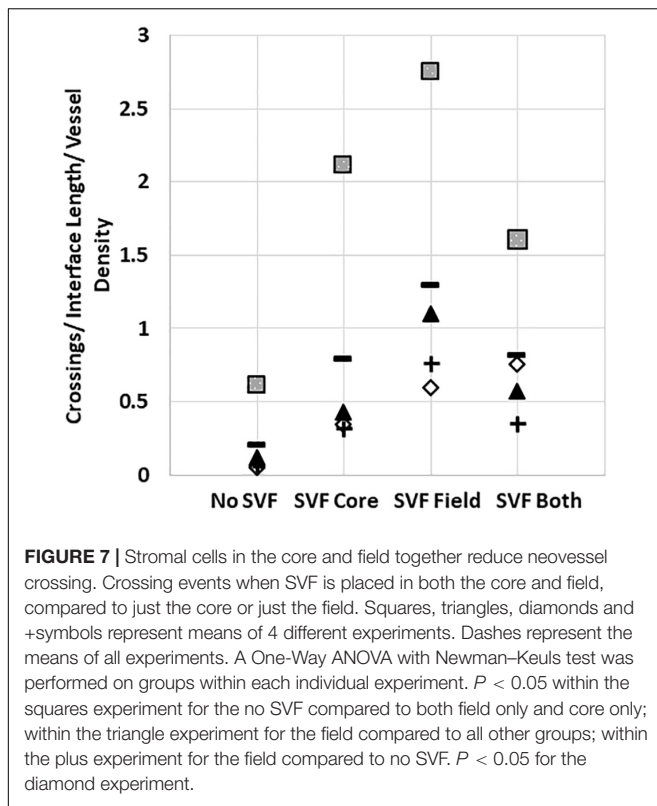


FIGURE 6 | Effect of VEGF-A on neovessel invasion. Effect of a VEGF trap on (A) interface crossings and (B) vessel density, compared SVF alone and a control IgG chimera protein. (C) Normalized neovessel invasion and (D) vessel density in CIF constructs containing microvessels alone or microvessels with recombinant VEGF-A₁₆₅ added to the media (+VEGF). One Way ANOVA with Newman-Keuls test (A,B) or Student's *t*-test (C,D). Bars are mean \pm SEM, *N* = 5. **P* < 0.05 compared to all other groups.

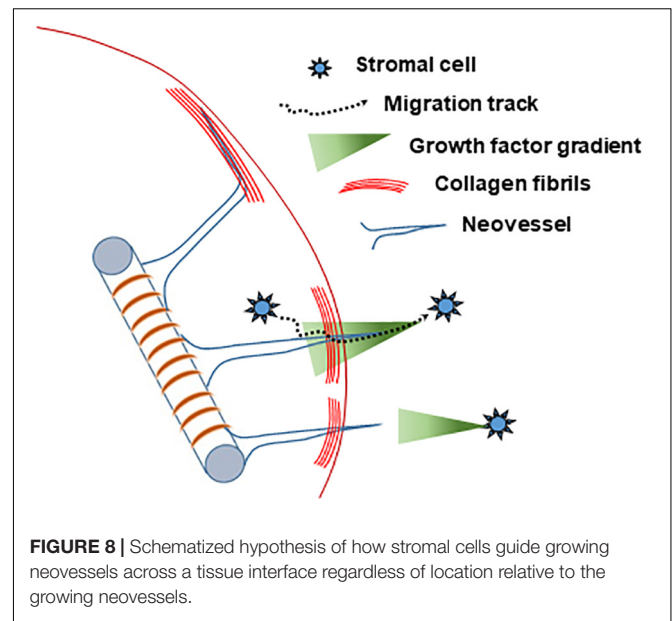
crossing. When measured, however, collagen density at the interface or areas adjacent to the interface did not change significantly in the presence of MVs, or MVs and SVF cells, over 10 days when compared to acellular constructs. Nor did we observe gross collagen remodeling or degradation by SEM, despite small holes where cells or vessels had crossed. This suggests that neither the MVs nor the stromal cells are grossly degrading collagen fibrils or altering fibril density along the interface. Given the strong dependence of neovessel growth on collagen fibrils, and the absence of gross fibril remodeling, there is likely a different mechanism responsible for neovessel crossing. However, we cannot completely rule out that the SVF made subtle changes to the interface that we were unable to detect. Regardless of whether SVF cell-induced structural changes are present in the interface, some instruction by the stromal cells is required for the growing neovessels to ignore the deflecting contact guidance cues at the interface. For example, cell contraction during migration can form a long-range stiffness gradient in 3D native matrices (Rivron et al., 2012; Han et al., 2018). Such differences in stiffness could further influence fibril-neovessel interactions, affecting neovessel growth and branching during angiogenesis (Edgar et al., 2014b; Underwood et al., 2014). While this is a possible mechanism of instruction by the stromal cells in the bulk phase collagen gel, it seems unlikely that such a phenomenon is directing neovessel growth across the densely packed interface.

Spatially positioned biochemical factors (i.e., gradients) seemed the most likely factor to provide long distance directional cues during angiogenesis. They are known to do this by creating zones of pro-angiogenic signals as well as instructing neovessel orientation via tip-stalk cell dynamics (Gerhardt et al., 2003; Hellstrom et al., 2007; Morris et al., 2015). Furthermore, the matrix-binding ability of nearly all these angiogenic factors results in spatial zones or tracks of angiogenic signals that a neovessel tip cell could detect and track as it moves through tissue compartments. The spatial arrangement of angiogenic factor-driven guidance cues can arise from either matrix architecture (porosity, anisotropy of fibrils and solute diffusion) and/or ligand distribution (heparan sulfate proteoglycans, integrins, etc.). This implies that the sources of these factors within the relevant tissue compartment must be under some local control as the ubiquitous release of factors would not give rise to such gradients, but rather a homogenous distribution. Stromal vascular fraction cells produce angiogenic factors and their heterogeneous spatiotemporal distribution within the tissue may provide the opportunity to create these spatially defined biochemical guidance cues.

Consistent with this idea, sequestration of SVF cell-produced VEGF-A, a known angiogenic factor and guidance cue for neovessels (Gerhardt and Betsholtz, 2005; Ahmed and Bicknell, 2009), largely reduced neovessel invasion. Interestingly, the ubiquitous presence of VEGF-A in the absence of SVF cells was



not sufficient to promote neovessel invasion. This suggests that VEGF-A signaling may need to be presented to the growing neovessel as a spatiotemporal gradient (which is not the case when ubiquitously added to the culture) for neovessels to cross the interface; such gradients are necessary in VEGF-A regulated tip-stalk cell behavior (Chappell et al., 2011). The mechanism by which VEGF-A instructs neovessels to overcome collagen fibril durotaxis and contact guidance and cues at the interface is unclear. Whether VEGF-A regulates proliferation or migration, both of which are necessary for angiogenesis (Rauff et al., 2019), during interface crossing is unclear. Given that exogenous VEGF-A promoted overall angiogenesis in our model, and thus both proliferation and migration, but not neovessel guidance, it is likely another VEGF-dependent activity is relevant. One possibility is that differential signaling by VEGF-A receptors may be playing a role. For example, deletion of the neuropilin-1 (Nrp-1) gene in mice results in the inability of neovessels to cross laterally into neighboring tissue compartments in the developing mouse hindbrain (Gerhardt et al., 2004), a tissue dynamic similar to that modeled in our experiments. Nrp-1 is a receptor expressed on neovessel tip cells that binds the VEGF-A₁₆₅ isoform, contributing to neovessel guidance in coordination with VEGF Receptor 2 (VEGFR2; Gerhardt et al., 2003; Zachary, 2011). Alternatively, changes in matrix architecture near the interface may induce differential mechanoregulation of VEGF signaling members. Sprout polarization and reorientation in response to VEGF signaling slows with increasing collagen density unless a higher magnitude VEGF gradient is introduced (Shamloo et al., 2012). Such a phenomenon could partially explain the different



magnitude in crossing observed when SVF cells are included in the field rather than the core. Fibril alignment secondary to matrix deformation has been shown to increase VEGFR2 expression, potentially enhancing the angiogenic response of neovessels (Rivron et al., 2012). Whether similar dynamics are contributing to neovessel interface deflection and invasion in our system remains to be determined.

Based on our collective findings (summarized in **Table 1**) and the above discussed considerations, we propose the following working model of neovessel invasion across tissue interfaces (**Figure 8**). Stromal cells, which freely move between tissue compartments, establish spatial gradients of VEGF, which guide neovessels across the interface. A key element of this hypothesis is the spatiotemporal position of the stromal cell relative to the neovessels and the interface, and, consequently, the spatiotemporal orientation of a VEGF-A guidance cue. When stromal cells are located opposite the growing vessels (i.e., in the field), soluble VEGF-A will naturally form a gradient as it diffuses through the collagen toward the core. When stromal cells are in the core only, the cells may be secreting or depositing a gradient of VEGF-A as they migrate through the interface and into the field. This cellular migration was confirmed via Hoechst staining, which showed a larger number of cells migrating into the field when SVF was seeded in the core, compared to controls without SVF. A larger increase in neovessel crossing events was observed when stromal cells were in the field region, rather than mixed together with MVs in the core, suggesting a large diffusion guidance cue from the field SVF exists. This large field-derived diffusion gradient is decreased when cells were seeded on both sides of the interface. This leaves only local gradients established by cells migrating from the core into the field. As only a portion of the cells in the core will cross the interface, the total crossing event is fewer than when SVF is in the field only. Therefore, there are likely two types of guidance cues derived by stromal cells: large angiostatic gradients that guide over longer distances

TABLE 1 | Summary of neovessel invasion findings.

Experimental condition	Key observations	Conclusion/Implication
Neovessels alone	Neovessels do not cross interface	
Neovessels + SVF in core	Neovessels cross interface	Stromal cells promote neovessel invasion
Neovessels + SVF in field	Neovessels cross interface	
SVF in collagen gels	Express VEGF-A	VEGF-A presence is necessary but not sufficient for SVF-enabled neovessel invasion
Neovessels + SVF + anti-VEGF	Neovessels do not cross interface	
Neovessels + recombinant VEGF	Neovessels do not cross interface	
SHG of fibril architecture	Fibrils at interface are dense	Deflection of neovessels at the interface is due to collagen fibril density at the interface.
Simulation: increased interface density	Neovessels do not cross interface	
Simulation: fibril alignment at interface	Neovessels cross interface without high initial density	

and local cell-derived guidance tracks. Given that VEGF-A is present as different isoforms with differing abilities to bind matrix, it is likely that gradients consist of both bound and freely diffusible VEGF-A. Each aspect of these gradients may potentially contribute differently to the guidance cues sensed by the neovessels, thus gradients produced in the core and field may not have equal effects.

Tissue vascularization is important for ischemic tissue repair, wound healing, regenerative medicine, and in many pathologies. In all cases, tissue boundaries exist that could impede integration of the new vasculature into the existing circulation. This is particularly relevant in applications involving grafts and tissue implants where discrete implant and recipient-site boundaries are present. Consequently, solutions facilitating the guidance of neovessels across tissue interfaces would significantly advance vascularization-dependent therapies and tissue vascularization strategies. Our evidence suggests that the stromal cells, normally resident within tissues, play a key role in promoting tissue vascularization and could be leveraged to facilitate vascularization, or, alternatively, targeted to stop vascularization in pathology. In fact, many of the cells used in adult cell therapies, due to pro-vascular capabilities intrinsic to the cells (Moon et al., 2006; Traktuev et al., 2008; Morris et al., 2015), promote tissue vascularization. In this context, the core in our model represents an idealized tissue implant in which a preformed, angiogenic vasculature is implanted into a relatively low density, quiescent vascular environment. This is because angiogenic vascular beds tend to produce a high number of neovessels, which will over time be pruned and remodeled as the vascular bed matures. In the case of our CIF, we have simplified the model to a more extreme scenario where the implant site (i.e., the field) is avascular. Our results suggest that incorporation of stromal cells in the tissue implant (i.e., the core) and/or delivery of stromal cells to the implant site (i.e., the field), whichever is more feasible, would facilitate vascularization and engraftment of the implant.

DATA AVAILABILITY STATEMENT

The raw data supporting the conclusions of this article, as well as the input files used for the simulations, will be made available by the authors, without undue reservation. The open-source FEBio

software used for the simulations is available at www.febio.org. The AngioFE plugin for FEBio used for the simulations is available at www.febio.org/plugins/.

ETHICS STATEMENT

The animal study was reviewed and approved by Dartmouth College IACUC.

AUTHOR CONTRIBUTIONS

LK and JH designed the core-in field model. HS and JH designed the experiments. HS, JD, LK, NB, and JB performed the experiments and data analysis. NB developed the image analysis algorithms used to assess microvessel density. AR, HS, KA, and SL performed the structural imaging and analysis. AP, KA, SL, and JW designed the computational framework. SL designed and performed the computational simulations. LK, SL, HS, AR, JW, and JH wrote and edited the manuscript. All authors contributed to the article and approved the submitted version.

FUNDING

Research reported in this publication was supported by the National Institutes of Health under award numbers R01HL131856, R01GM083925, and R01AR069297. The content is solely the responsibility of the authors and does not necessarily represent the official views of the National Institutes of Health.

ACKNOWLEDGMENTS

SEM images of collagen microstructure were collected at the University Instrumentation Center (UIC) at the University of New Hampshire in Durham, NH with the help of Nancy Cherim. Microscopy equipment at UNH was obtained using a NCR Shared Equipment Grant # 1S10RR024761-01. Additional confocal imaging occurred within the Cell and Tissue Imaging and Histology Core at the Kentucky Spinal Cord Injury Research Center at the University of Louisville. The authors also gratefully acknowledge Dr. Matthew Weitzman from

Olympus, and Dr. Mark Townley from the University of New Hampshire UIC, for assistance with confocal imaging. Second harmonic generation imaging was performed at the Fluorescence Microscopy Core Facility, a part of the Health Sciences Cores at the University of Utah.

REFERENCES

- Ahmed, Z., and Bicknell, R. (2009). Angiogenic signalling pathways. *Methods Mol. Biol.* 467, 3–24. doi: 10.1007/978-1-59745-241-0_1
- Altalhi, W., Sun, X., Sivak, J. M., Husain, M., and Nunes, S. S. (2017). Diabetes impairs arterio-venous specification in engineered vascular tissues in a perivascular cell recruitment-dependent manner. *Biomaterials* 119, 23–32. doi: 10.1016/j.biomaterials.2016.12.003
- Bordeleau, F., Mason, B. N., Lollis, E. M., Mazzola, M., Zanotelli, M. R., Somasegar, S., et al. (2017). Matrix stiffening promotes a tumor vasculature phenotype. *Proc. Natl. Acad. Sci. U.S.A.* 114, 492–497. doi: 10.1073/pnas.1613855114
- Breier, G. (2000). Angiogenesis in embryonic development—a review. *Placenta* 21(Suppl. A), S11–S15.
- Chang, C. C., Krishnan, L., Nunes, S. S., Church, K. H., Edgar, L. T., Boland, E. D., et al. (2012). Determinants of microvascular network topologies in implanted neovasculatures. *Arterioscler. Thromb. Vasc. Biol.* 32, 5–14. doi: 10.1161/atvbaha.111.238725
- Chappell, J. C., Wiley, D. M., and Bautch, V. L. (2011). Regulation of blood vessel sprouting. *Semin. Cell. Dev. Biol.* 22, 1005–1011. doi: 10.1016/j.semcdb.2011.10.006
- Edgar, L. T., Hoying, J. B., Utzinger, U., Underwood, C. J., Krishnan, L., Baggett, B. K., et al. (2014a). Mechanical interaction of angiogenic microvessels with the extracellular matrix. *J. Biomech. Eng.* 136:021001.
- Edgar, L. T., Hoying, J. B., and Weiss, J. A. (2015a). In silico investigation of angiogenesis with growth and stress generation coupled to local extracellular matrix density. *Ann. Biomed. Eng.* 43, 1531–1542. doi: 10.1007/s10439-015-1334-3
- Edgar, L. T., Maas, S. A., Guilkey, J. E., and Weiss, J. A. (2015b). A coupled model of neovessel growth and matrix mechanics describes and predicts angiogenesis in vitro. *Biomech. Model. Mechanobiol.* 14, 767–782. doi: 10.1007/s10237-014-0635-z
- Edgar, L. T., Sibole, S. C., Underwood, C. J., Guilkey, J. E., and Weiss, J. A. (2012). A computational model of in vitro angiogenesis based on extracellular matrix fibre orientation. *Comput. Methods Biomech. Biomed. Engin.* 16, 790–801. doi: 10.1080/10255842.2012.662678
- Edgar, L. T., Underwood, C. J., Guilkey, J. E., Hoying, J. B., and Weiss, J. A. (2014b). Extracellular matrix density regulates the rate of neovessel growth and branching in sprouting angiogenesis. *PLoS One* 9:e85178. doi: 10.1371/journal.pone.0085178
- Folkman, J. (1995). Angiogenesis in cancer, vascular, rheumatoid and other disease. *Nat. Med.* 1, 27–31.
- Fraser, J. K., Wulur, I., Alfonso, Z., and Hedrick, M. H. (2006). Fat tissue: an underappreciated source of stem cells for biotechnology. *Trends Biotechnol.* 24, 150–154. doi: 10.1016/j.tibtech.2006.01.010
- Gerhardt, H., and Betsholtz, C. (2005). “How do endothelial cells orientate?” in *Mechanisms of Angiogenesis*, eds M. Clauss and G. Breier (Basel: Birkhäuser), doi: 10.1007/3-7643-7311-3_1
- Gerhardt, H., Golding, M., Fruttiger, M., Ruhrberg, C., Lundkvist, A., Abramsson, A., et al. (2003). VEGF guides angiogenic sprouting utilizing endothelial tip cell filopodia. *J. Cell Biol.* 161, 1163–1177. doi: 10.1083/jcb.200302047
- Gerhardt, H., Ruhrberg, C., Abramsson, A., Fujisawa, H., Shima, D., and Betsholtz, C. (2004). Neuropilin-1 is required for endothelial tip cell guidance in the developing central nervous system. *Dev. Dyn.* 231, 503–509. doi: 10.1002/dvdy.20148
- Grant, S. D., Yenisey, C., Rose, W. R., Tootell, M., Santra, M., and Iozzo, V. R. (2002). Decorin suppresses tumor cell mediated angiogenesis. *Oncogene* 21, 4765–4777. doi: 10.1038/sj.onc.1205595
- Gruionu, G., Stone, A. L., Schwartz, M. A., Hoying, J. B., and Williams, S. K. (2010). Encapsulation of ePTFE in prevascularized collagen leads to perimplant vascularization with reduced inflammation. *J. Biomed. Mater. Res. A* 95, 811–818. doi: 10.1002/jbm.a.32925
- Han, W., Chen, S., Yuan, W., Fan, Q., Tian, J., Wang, X., et al. (2016). Oriented collagen fibers direct tumor cell intravasation. *Proc. Natl. Acad. Sci. U.S.A.* 113, 11208–11213. doi: 10.1073/pnas.1610347113
- Han, Y. L., Ronceray, P., Xu, G., Malandrino, A., Kamm, R. D., Lenz, M., et al. (2018). Cell contraction induces long-ranged stress stiffening in the extracellular matrix. *Proc. Natl. Acad. Sci. U.S.A.* 115, 4075–4080. doi: 10.1073/pnas.1722619115
- Hellstrom, M., Phng, L. K., and Gerhardt, H. (2007). VEGF and Notch signaling: the yin and yang of angiogenic sprouting. *Cell Adh. Migr.* 1, 133–136. doi: 10.4161/cam.1.3.4978
- Hoying, J. B., Boswell, C. A., and Williams, S. K. (1996). Angiogenic potential of microvessel fragments established in three-dimensional collagen gels. *In Vitro Cell. Dev. Biol. Anim.* 32, 409–419. doi: 10.1007/bf02723003
- Hoying, J. B., Utzinger, U., and Weiss, J. A. (2014). Formation of microvascular networks: role of stromal interactions directing angiogenic growth. *Microcirculation* 21, 278–289. doi: 10.1111/micc.12115
- Kirkpatrick, N. D., Andreou, S., Hoying, J. B., and Utzinger, U. (2007). Live imaging of collagen remodeling during angiogenesis. *Am. J. Physiol. Heart Circ. Physiol.* 292, H3198–H3206.
- Koh, Y. J., Koh, B. I., Kim, H., Joo, H. J., Jin, H. K., Jeon, J., et al. (2011). Stromal vascular fraction from adipose tissue forms profound vascular network through the dynamic reassembly of blood endothelial cells. *Arterioscler. Thromb. Vasc. Biol.* 31, 1141–1150. doi: 10.1161/atvbaha.110.218206
- Krishnan, L., Underwood, C. J., Maas, S., Ellis, B. J., Kode, T. C., Hoying, J. B., et al. (2008). Effect of mechanical boundary conditions on orientation of angiogenic microvessels. *Cardiovasc. Res.* 78, 324–332. doi: 10.1093/cvr/cvn055
- Laschke, M. W., Harder, Y., Amon, M., Martin, I., Farhadi, J., Ring, A., et al. (2006). Angiogenesis in tissue engineering: breathing life into constructed tissue substitutes. *Tissue Eng.* 12, 2093–2104. doi: 10.1089/ten.2006.12.2093
- Luttun, A., Tjwa, M., and Carmeliet, P. (2003). Placental growth factor (PlGF) and its receptor Flt-1 (VEGFR-1): novel therapeutic targets for angiogenic disorders. *Ann. N. Y. Acad. Sci.* 979, 80–93. doi: 10.1111/j.1749-6632.2002.tb04870.x
- Maas, S. A., Ellis, B. J., Ateshian, G. A., and Weiss, J. A. (2012). FEBio: finite elements for biomechanics. *J. Biomech. Eng.* 134:011005.
- Maijib, J. G., Boyd, N. L., Dale, J. R., Hoying, J. B., Morris, M. E., and Williams, S. K. (2014). Concentration Dependent Vascularization of Adipose Stromal Vascular Fraction Cells. *Cell Transplant.* 24, 2029–2039. doi: 10.3727/096368914x685401
- Moon, M. H., Kim, S. Y., Kim, Y. J., Kim, S. J., Lee, J. B., Bae, Y. C., et al. (2006). Human adipose tissue-derived mesenchymal stem cells improve postnatal neovascularization in a mouse model of hindlimb ischemia. *Cell Physiol. Biochem.* 17, 279–290. doi: 10.1159/000094140
- Morris, M. E., Beare, J. E., Reed, R. M., Dale, J. R., LeBlanc, A. J., Kaufman, C. L., et al. (2015). Systemically delivered adipose stromal vascular fraction cells disseminate to peripheral artery walls and reduce vasomotor tone through a CD11b+ cell-dependent mechanism. *Stem Cells Transl. Med.* 4, 369–380. doi: 10.5966/sctm.2014-0252
- Nunes, S. S., Greer, K. A., Stiening, C. M., Chen, H. Y., Kidd, K. R., Schwartz, M. A., et al. (2010). Implanted microvessels progress through distinct neovascularization phenotypes. *Microvasc. Res.* 79, 10–20. doi: 10.1016/j.mvr.2009.10.001
- Nunes, S. S., Maijib, J. G., Krishnan, L., Ramakrishnan, V. M., Clayton, L. R., Williams, S. K., et al. (2013). Generation of a functional liver tissue mimic using adipose stromal vascular fraction cell-derived vasculatures. *Sci. Rep.* 3:2141.
- Ramakrishnan, V. M., Tien, K. T., McKinley, T. R., Bocard, B. R., McCurry, T. M., Williams, S. K., et al. (2016). Wnt5a regulates the assembly of human adipose derived stromal vascular fraction-derived microvasculatures. *PLoS One* 11:e0151402. doi: 10.1371/journal.pone.0151402
- Rauff, A., LaBelle, S. A., Strobel, H. A., Hoying, J. B., and Weiss, J. A. (2019). Imaging the dynamic interaction between sprouting microvessels and the extracellular matrix. *Front. Physiol.* 10:1011. doi: 10.3389/fphys.2019.01011

SUPPLEMENTARY MATERIAL

The Supplementary Material for this article can be found online at: <https://www.frontiersin.org/articles/10.3389/fphys.2020.01026/full#supplementary-material>

- Ravanti, L., and Kahari, V. M. (2000). Matrix metalloproteinases in wound repair (review). *Int. J. Mol. Med.* 6, 391–407.
- Rehman, J., Traktuev, D., Li, J., Merfeld-Clauss, S., Temm-Grove, C. J., Bovenkerk, J. E., et al. (2004). Secretion of angiogenic and antiapoptotic factors by human adipose stromal cells. *Circulation* 109, 1292–1298. doi: 10.1161/01.cir.0000121425.42966.f1
- Rivron, N. C., Vrij, E. J., Rouwkema, J., Le Gac, S., van den Berg, A., Truckenmuller, R. K., et al. (2012). Tissue deformation spatially modulates VEGF signaling and angiogenesis. *Proc. Natl. Acad. Sci. U.S.A.* 109, 6886–6891. doi: 10.1073/pnas.1201626109
- Shamloo, A., Xu, H., and Heilshorn, S. (2012). Mechanisms of vascular endothelial growth factor-induced pathfinding by endothelial sprouts in biomaterials. *Tissue Eng. Part A* 18, 320–330. doi: 10.1089/ten.tea.2011.0323
- Shepherd, B. R., Chen, H. Y., Smith, C. M., Gruionu, G., Williams, S. K., and Hoying, J. B. (2004). Rapid perfusion and network remodeling in a microvascular construct after implantation. *Arterioscler. Thromb. Vasc. Biol.* 24, 898–904. doi: 10.1161/01.atv.0000124103.86943.1e
- Shepherd, B. R., Hoying, J. B., and Williams, S. K. (2007). Microvascular transplantation after acute myocardial infarction. *Tissue Eng.* 13, 2871–2879. doi: 10.1089/ten.2007.0025
- Taufalele, P. V., Vanderburgh, J. A., Munoz, A., Zanotelli, M. R., and Reinhart-King, C. A. (2019). Fiber alignment drives changes in architectural and mechanical features in collagen matrices. *PLoS One* 14:e0216537. doi: 10.1371/journal.pone.0216537
- Traktuev, D. O., Merfeld-Clauss, S., Li, J., Kolonin, M., Arap, W., Pasqualini, R., et al. (2008). A population of multipotent CD34-positive adipose stromal cells share pericyte and mesenchymal surface markers, reside in a periendothelial location, and stabilize endothelial networks. *Circ. Res.* 102, 77–85. doi: 10.1161/circresaha.107.159475
- Underwood, C. J., Edgar, L. T., Hoying, J. B., and Weiss, J. A. (2014). Cell-generated traction forces and the resulting matrix deformation modulate microvascular alignment and growth during angiogenesis. *Am. J. Physiol. Heart Circ. Physiol.* 307, H152–H164.
- Utzinger, U., Baggett, B., Weiss, J. A., Hoying, J. B., and Edgar, L. T. (2015). Large-scale time series microscopy of neovessel growth during angiogenesis. *Angiogenesis* 18, 219–232. doi: 10.1007/s10456-015-9461-x
- Williams, S. K. (1995). Endothelial cell transplantation. [Review] [42 refs]. *Cell Transplant.* 4, 401–410. doi: 10.1016/0963-6897(95)00023-q
- Yoshimura, K., Sato, K., Aoi, N., Kurita, M., Hirohi, T., and Harii, K. (2008). Cell-assisted lipotransfer for cosmetic breast augmentation: supportive use of adipose-derived stem/stromal cells. *Aesthetic Plast. Surg.* 32, 48–55. doi: 10.1007/s00266-007-9019-4
- Zachary, I. C. (2011). How neuropilin-1 regulates receptor tyrosine kinase signalling: the knowns and known unknowns. *Biochem. Soc. Trans.* 39, 1583–1591. doi: 10.1042/bst20110697
- Zimmerlin, L., Donnenberg, V. S., Pfeifer, M. E., Meyer, E. M., Peault, B., Rubin, J. P., et al. (2010). Stromal vascular progenitors in adult human adipose tissue. *Cytometry A* 77, 22–30.

Conflict of Interest: JH is a partner at Advanced Solutions Life Sciences, which commercializes the microvessel technology. The commercial activity of ASLS is outside the scope of the submitted work.

The remaining authors declare that the research was conducted in the absence of any commercial or financial relationships that could be construed as a potential conflict of interest.

Copyright © 2020 Strobel, LaBelle, Krishnan, Dale, Rauff, Poulson, Bader, Beare, Aliaj, Weiss and Hoying. This is an open-access article distributed under the terms of the Creative Commons Attribution License (CC BY). The use, distribution or reproduction in other forums is permitted, provided the original author(s) and the copyright owner(s) are credited and that the original publication in this journal is cited, in accordance with accepted academic practice. No use, distribution or reproduction is permitted which does not comply with these terms.